12,03

Space-Charge-Limited Efficiency of Electrically-Injected Carriers Localization

© N.I. Bochkareva, Y.G. Shreter¶

Ioffe Institute,
St. Petersburg, Russia

¶ E-mail: y.shreter@mail.ioffe.ru

Received September 5, 2022
Revised September 5, 2022
Accepted: September 6, 2022

The mechanism for the influence of defects in the GaN on the efficiency of localization of electrically-injected charge carriers in the InGaN|GaN quantum well is studied using tunnel spectroscopy of deep centers. It is found that the curves of the quantum efficiency and the spectral efficiency of radiative recombination dependencies on forward bias have the shape with maximum and humps at the biases corresponding to the impurity bands of color centers in GaN. The quantum efficiency droop with increasing bias is accompanied by a blue shift of the emission spectrum. We explain these effects based on the model of carrier localization in the quantum well, which takes into account the significant contribution to the tunneling transparency of the potential walls of the quantum well from ionized deep centers and their recharging with increasing forward bias.

Keywords: gallium nitride, quantum well, charge carrier localization, tunneling, quantum effeciency, color centers.

DOI: 10.21883/PSS.2023.01.54987.458

1. Introduction

Light-emitting p−n-nanostructures based on GaN, which are the basic element of solid-state lighting sources [1,2], have high efficiency, despite the huge density of lattice structural defects, point defects and their complexes responsible for „dirty“ the GaN band gap ($E_{g,\,\mathrm{GaN}} = 3.42$ eV at 300 K) with a deeper distribution of localized states [3,4] than in amorphous Si. However, the main physical question is to what extent the key problems of nitride optoelectronics are related to defects [2], and first of all, the problems of quantum efficiency droop with increasing power and radiated wavelength of nanostructures with InGaN|GaN quantum wells, are still insufficiently studied.

Already in early experimental studies, it was shown that the high density of localized states created by defects in the GaN band gap facilitates tunneling through potential barriers in the GaN, and sub-barrier tunneling is the main mechanism for the passage of current in light-emitting and photovoltaic nanostructures, as well as in the gates of field-effect transistors based on GaN [5–7]. The dependences of the tunnel current on the forward bias are usually considered using an approach developed to describe the excess current in Esaki tunnel junctions [8]. This approach is based on the assumption that the rate of tunneling charge transfer at the given bias linearly depends on the density of empty final states at the tunnel transport level at the boundary of the p−n-junction, and the shape of the volt-ampere characteristic of the tunnel structure reflects the energy distribution of the density of localized states in a less doped transition region. In the case of a high density of deep centers, however, it is necessary to take into account the dependence of the tunneling probability on the electric field strength in the barrier, which decreases with increasing forward bias due to recharging of deep centers and a corresponding decrease in the volume charge density. In the epitaxial layers of GaN, in addition to impurity Urbach tails of states exponentially falling into the band gap, there are several types of color centers responsible for wide Gaussian bands of intracenter optical absorption and photoluminescence (PL) in GaN [9–11]. In the p−n-nanostructures, deep color centers ionized at the boundaries with the InGaN|GaN quantum well make a significant contribution to the equilibrium volume charge density and electric field strength at the boundaries, which increases the tunneling permeability of the potential walls of the quantum well.

As our recent measurements of tunneling current and photocurrent with optical excitation of p−n-structures with a single InGaN|GaN quantum well have shown, with optical injection, a decrease in the tunneling permeability of the well walls as a result of recharging of the color centers as the forward bias increases leads to an increase in localization efficiency carriers in the quantum well, which manifests itself in a stepwise increase in the efficiency of PL from the quantum well and a red shift of the spectrum of PL [12]. The purpose of this work is to study the mechanism of the influence of deep centers on the efficiency of carrier localization in a quantum well and the quantum efficiency of electroluminescence (EL) in p−n-structures with InGaN|GaN quantum wells during electrical injection.

2. Experiment

The studies were carried out on light-emitting p−n-nanostructures of the same types as in [12], designated as A and B, with a single InGaN|GaN quantum well with a thickness of 30 Å, peak energy EL $h\nu_p = 2.65$ eV ($\lambda_p = 465$ nm) at rated current $I = 20$ mA (area of structures 10^{-3} cm^2) and the maximum internal quantum efficiency of EL, which is 60 and 40% in the structures A and B, respectively. The structure details are shown in [12-14]. According to measurements of the capacitance-voltage characteristics showed, *n*- and *p*-regions in nanostructures A are heavily doped ($> 3 \cdot 10^{18}$ cm^{-3}), but in the *n*-GaN layer there is a weakly doped ($7 \cdot 10^{16}$ cm^{-3}) region with the width of ~ 120 nm bordering on the quantum well. In the nanostructures B n-region is doped much more strongly (10^{18} cm^{-3}) than p-area ($\sim 2 \cdot 10^{17}$ cm^{-3}).

Measurements of current tunneling spectra of — current as a function of the forward bias of p−n-junction in energy units V (equivalent to the difference between the electron and hole Fermi levels $F_n - F_p$), conducted using a Keithley 238 current and voltage meter source. The forward bias of the p−n-junction $V = q(V_f - Ir_s)$ was determined taking into account the drop in the applied forward voltage V_f on the series resistance of the structure r_s, assumed to be equal to the differential resistance dV_f/dI at rated current $I = 20$ mA and amounting to structures A and B 14.5 and 8.2 Ω, respectively. The EL spectra were recorded on the spectrometer AvaSpec-2048.

3. Experimental results and discussion

3.1. The tunneling conductivity of a potential barrier in GaN

The high density of lefects in GaN facilitates tunneling, and with direct biases, the main carrier flows in the p−n-nanostructure move towards the quantum well due to hopping diffusion near the electron and hole tunnel transport levels, $E_{tn} = F_n$ and $E_{tp} = F_p$ (Fig. 1). The rate of tunneling charge transfer through the n- and p-barriers limit the boundary layers (walls of the quantum well) with the highest localization energy and the lowest density of local centers along the tunneling length. The tunnel resistance of the boundary layer in the p-barrier (layer thickness d in Fig. 1) is significantly higher than in the n-barrier, due to the large effective mass of holes in the GaN, as well as due to the asymmetry of the degrees of doping and energy spectra of defects in the layers of GaN p- and n-type. A direct experimental confirmation of this conclusion, first of all, is the fact that in typical nanostructures with multiple InGaN|GaN quantum wells, only the quantum well closest to the p-region emits light [15]. With forward biases, the tunneling flow of holes is limited by the low tunneling permeability of the p-barrier, and the number of electrons required to fulfill the local quasi-neutrality

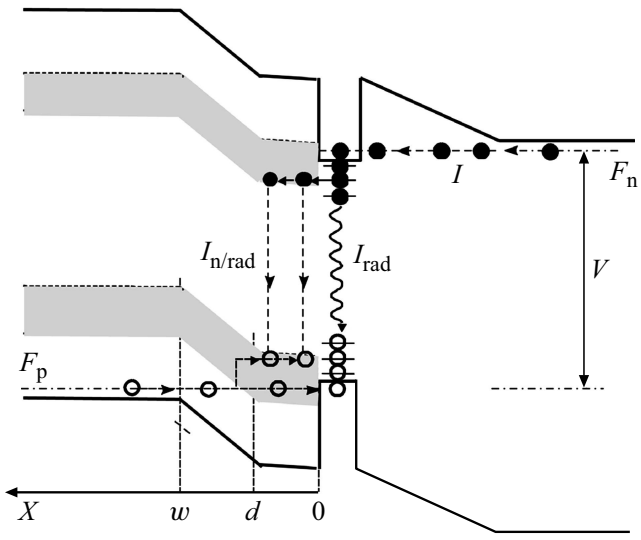

Figure 1. Scheme of energy bands p−n-structures with an InGaN|GaN quantum well at forward bias $V > h\nu_p$.

condition is provided by the higher tunneling permeability of the n-barrier.

The deep quasi-continuous distribution of localized states in the GaN band gap, which lattice structural defects, point defects and their complexes create in epitaxial layers, can be represented as a superposition of impurity Urbach tails of states and Gaussian bands of color centers forming impurity bands in the upper and lower halves of the GaN band gap [9–11].

According to the model of tunneling through local centers in Esaki junctions [16], the excess tunneling current through the potential barrier is proportional to the product of the tunneling permeability of the barrier $D(E_t)$, the density of occupied initial states $\rho_s(E_t)$ and the total density empty final states$\rho_s(E_t)$ of the impurity $\rho_{if}(E_t)$ and the Urbach tail $\rho_{Uf}(E_t)$ at the tunnel transport layer E_t near the heteroboundary, $\rho_f(E_t) = \rho_{if}(E_t) + \rho_{Uf}(E_t)$:

$$I \propto D(E_t)\rho_s(E_t)\big(\rho_{if}(E_t) + \rho_{Uf}(E_t)\big). \qquad (1)$$

The tunneling permeability of a triangular potential barrier, which determines the probability of tunneling a charge carrier from an occupied initial state with energy E_t to an empty final state with the same energy, calculated by Keldysh [17], in its simplest form equals

$$D = \exp\left(-\frac{\pi\delta}{2\sqrt{2\hbar}}\sqrt{2m^*(V_0 - V)}\right), \qquad (2)$$

where V_0 and $\delta = (V_0 - V)/qF_b$ — barrier height and width, V — is the forward bias, $F_b = ((V_0 - V)qN/\varepsilon)^{1/2}$ — electric field strength, q — electron charge, ε — permittivity, m^* — reduced effective mass of electron and hole, $N = N_t + N_{Ut} + N_{Gt}$ — total concentration of ionized impurity centers of the main dopant N_t, the Urbach tail N_{Ut} and the color centers $N_{Gt} = \Sigma_i \rho_{it}(E)$.

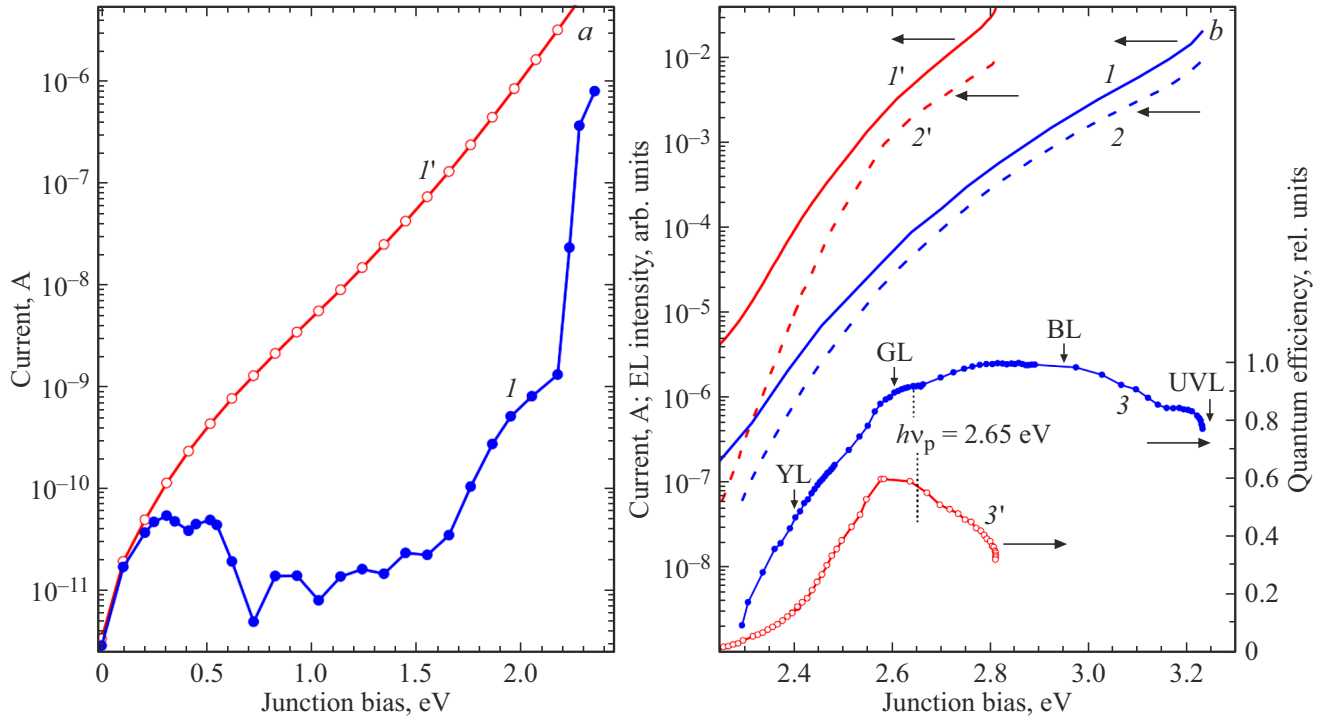

Figure 2. Dependences on the forward bias p–n of the current $(1, 1')$ in the region of the bias $V < V_{th}$ (a) and $V > V_{th}$ (b), intensity $(2, 2')$ and the quantum efficiency of EL $(3, 3')$ (b) for structures A $(1–3)$ and B $(1'–3')$. The arrows mark the peak energies of the optical absorption bands YL-, GL-, BL-centers and the peak energy of the ultraviolet (UVL) PL in GaN (b).

As the forward bias increases, the transport level E_t in a barrier with high tunneling resistance, moving to the edge of the allowed zone, crosses the impurity zone on the heteroboundary with a quantum well, the nature of the change in tunneling conductivity is mainly influenced, according to (2), by the change in the product two functions, $\rho_f(E_t)$ and $D(E_t)$:

$$g_{tun}(E_t) \propto D\left(\frac{d\rho_{if}}{dE_t} + \frac{d\rho_{Uf}}{dE_t}\right) + (\rho_{if} + \rho_{Uf}) \cdot \frac{dD}{dE_t}. \qquad (3)$$

According to (3), the increments of the density of empty finite states $d\rho_f(E_t)/dE_t$ when moving the level E_t lead to the greater increase g_{tun}, the higher the permeability of the barrier. But simultaneous filling and recharging of the final states of the impurity zone $\rho_i(E)$ leads to a weakening of the electric field strength and a decrease in permeability $(dD/dE_t < 0)$. Recharging the deep states of the exponential tail $\rho_U(E_t)$ does not lead to a significant decrease in permeability, since the full charge of its ionized states is determined by the density of small states.

3.2. Tunneling spectroscopy of deep centers at pre-threshold biases, $V < V_{th}$

Fig. 2, *a* shows the current-voltage characteristics of the nanostructures A and B, measured in the biases region less than the threshold bias of the detection of EL V_{th}. The shape of the curve for the nanostructure A (curve *1*) resembles similar characteristics of semiconductor tunnel junctions, in which, in addition to the tunnel peak associated with interband tunneling, there are humps of excess tunneling current caused by tunnel junctions through impurity levels.

The maximum and humps on the tunneling spectrum of the current $I(V)$ structure A clearly indicate the presence in the GaN band gap of several impurity of the Gaussian type $\rho_i(E)$ with biases maxima at $E_t = E_{0i}$ superimposed on the background of impurity states of the exponential Urbach tail $\rho_U(E)$. The double maximum of the tunnel current at low biases is caused by the presence of a Gaussian impurity$\rho_1(E_t)$.

The first maximum is associated with the maximum of the Gaussian $\rho_{1f}(E_t)$ at the level E_t. The appearance of an additional maximum and a region with negative differential conductivity on the $I–V$ characteristic is associated with an increase in the density $\rho_{Uf}(E_t)$ on the decline of the Gaussian $\rho_{1f}(E_t)$ and a decrease in tunnel permeability $D(E_t)$ as a result of a decrease in the space charge as the states $\rho_1(E_t)$ recharge. Sequential recharging of the impurity zone states as the bias increases leads to a stepwise decrease in the permeability, causing the formation of a valley of the $I–V$-characteristic, which indicates a significant contribution of the space charge of the color centers to the total space charge in the structure of A.

The equality of currents in structures A and B at small biases indicates the approximate equality of the density of states $\rho_1(E)$ in them. But in the region of biases

corresponding to the valley of the $I-V$-characteristic in structure A, only a weak depression is observed in structure B on the curve $\lg I(V)$ (curve I'), which indicates the predominant contribution of the Urbach tail states to the full charge in the structure B.

3.3. Effect of tunneling permeability of potential walls of a quantum well on efficiency of injection of charge carriers into a quantumwell, $V \geq V_{th}$

Fig. 2, *b* compares the $V \geq V_{th}$ dependences measured in the bias region of the current I (curves *1, 1′*) and the emission intensity I_{EL} (curves *2* and *2′*), represented on a semi-logarithmic scale, as well as the quantum efficiency of EL $\eta = I_{EL}/I$ (curves *3* and *3′*), represented on a linear scale, for the nanostructures A and B. As can be seen from Fig. 2, *b*, in both structures the curves $\lg I(V)$ and $\lg I_{EL}(V)$ have *S*-shaped, the curves $\eta(V)$ have a characteristic of light-emitting nanostructures based on GaN maximum. In the bias region $V_p > V > V_{th}$, the radiation intensity increases faster than the current and the efficiency increases with the bias. Efficiency peaks at peak biases of $V_p = 2.81$ and 2.58 eV and peak currents $I_p = 0.48$ and 2.2 mA in structures A and B, respectively, when the slopes of the curves $\lg I(V)$ and $\lg I_{EL}(V)$ become the same. In the region $V > V_p$, the current grows faster than I_{EL}, and the efficiency decreases with increasing bias. In addition to the maximum, the curves $\eta(V)$ for the structures A and B reveal a thin structure with kinks (convexity or concavity of the curves) in the region of the same biases.

As can be seen from Fig. 2, *b*, the EL spectrum from the quantum well begins to be detected at an bias $V_{th} = 2.3\,\text{eV} < h\nu_p$, when the main current flows „under" the quantum well and is a tunnel leakage current, and the over-barrier injection current into the quantum well is negligible, and recombination radiation in the well occurs due to tunnel injection of thermally activated carriers into the quantum well through the potential walls of the well.

The intensity of EL I_{EL} in the structures A and B slowly increases with the bias, increasing by 5 orders of magnitude at $V = 3.24$ and 2.81 eV, respectively, whereas with over-barrier injection into a quantum well, the radiation intensity should increase with the bias as $I_{EL} \propto \exp(V/nkT)$, $n = 1$, and at threshold bias $V_{th} = 2.3\,\text{eV}$ should increase by 5 orders of magnitude already at the bias $V = 2.6\,\text{eV}$. Exponential growth of I_{EL} with characteristic energy equal to or close to kT in the structures A and B is observed only near V_{th}, amounting to kT and $1.25\,kT$, respectively. This assumes that a significant proportion of the forward bias falls on the tunnel resistance of the well wall in the p-barrier.

The found features of the behavior of the current and emission intensity with increasing forward bias allow us to propose a model linking the efficiency of localization and radiative recombination of carriers in a quantum well with the density of the space charge in the walls of the well and its change as the forward bias increases and the tunnel transport levels E_{tp} and E_{tn} moves to the edges of free zones bands.

At forward biases of $h\nu_p \geq V > V_{th}$, the tunneling current into the quantum well is created by the main carriers capable of overcoming the injection barrier with a height of $E_{eff} = h\nu_p$. Since the concentrations of the main carriers at the boundaries of the space charge layers are determined by the Boltzmann distribution, as long as $V \leq h\nu_p$, the main current into the quantum well is created by carriers thermally activated to the top of the lowered injection barrier $E_{eff} = h\nu_p$. At forward biases $V > h\nu_p$, the main current into the quantum well flows near the tunnel transport levels E_{tn} and E_{tp} ($E_{tn} - E_{tp} = V$). In a time shorter than the radiative recombination time in the quantum well τ_r, the injected carriers are thermalized into the states of the quantum well tails and can recombine radiatively or tunnel to localized isoenergetic states in the opposite barrier and recombine nonradiatively in the well wall or tunnel through the wall. Due to the small thickness of the quantum well compared to the thickness of the walls of the well, it can be assumed that the carriers recombine non-radiatively, mainly in the walls of the well. The efficiency of localization and radiative recombination of carriers in a quantum well can be written in the following form:

$$\eta(V) = \frac{I_{rad}}{I_{rad} + I_{n/rad}} = \frac{\tau_{nr}}{\tau_r + \tau_{nr}}, \qquad (4)$$

where I_{rad}, $I_{n/rad}$ — are currents caused by radiative recombination in a quantum well and tunneling from a quantum well, respectively; $\tau_{n/r} = (1/\tau_{QW\to w} + 1/\tau_{QW\to p})^{-1}$ — the lifetime of carriers in localized states in the wall of a quantum well, determined by the time of nonradiative recombination in the wall of the well $\tau_{QW\to w}$ and the time of tunneling through the wall by jumps between local centers $\tau_{QW\to p}$.

At low injection levels, the differential resistance of the injection barrier E_{eff}, inversely proportional to the current I_{rad} and equal to $r_{eff} = kT/qI_{rad}$, is greater than the sequential differential tunneling resistances of potential well walls. The forward voltage drops almost entirely at the injection barrier E_{eff}, lowers its height and increases the tunneling currents of holes and electrons into the quantum well. This is reflected in the rapid increase in the intensity of radiation from the quantum well ($I_{EL} \propto I_{rad}$) near the threshold bias.

With an increase in the forward bias and the injection level, the resistance of r_{eff} decreases, and an increasing part of the bias increment falls on the tunnel resistance of the quantum well wall in the p-barrier r_w, slowing down the decrease barrier E_{eff} and straightening bands in the wall. The greater the straightening of the bands in the well wall, the greater the number of isoenergetic states with occupied non-basic carriers, electrons, and tail states in the quantum well, and the greater the tunneling flow of electrons from the quantum well, which leads to a slowdown in the growth of $I_{EL}(V)$ and $\eta(V)$ with the bias increase.

The efficiency increases, while $r_{\text{eff}}/r_{\text{w}} > 1$. But when, with the bias increase, the differential resistances of the injection barrier and the well wall become equal, the flow of electrons tunneling from the quantum well begins to increase as the bias increases faster than the flow of electrons radiatively recombining in the well, which leads to the efficiency droop. The maximum efficiency condition can be written as the equality $r_{\text{w}} = kT/qI_{\text{rad}}$ or $I_{\text{rad}} = kT/r_{\text{w}}$. The maximum efficiency in light-emitting nanostructures based on GaN is usually observed at a current density of the order 1 A/cm^2. For a structure with an area of $S = 10^{-3}$ cm^2 at peak current $I_{\text{p}} = 1$ mA, $r_{\text{w}} = kT/qI_{\text{p}} = 26\,\Omega$; at rated current $I = 20$ mA, $r_{\text{eff}} = kT/qI_{\text{rad}} = 1.3\,\Omega$.

3.4. The effect of the recharge of the color centers on the localization efficiency of injected carriers in the quantum well

The curve $\eta(V)$ for the nanostructure A has convexities (humps) in the vicinity of the biases $V = 2.4$ and 2.6 eV corresponding to the maxima of the Gaussians $\rho_{\text{YL}}(E)$ and $\rho_{\text{GL}}(E)$ responsible for the bands of yellow (YL) and green (GL) PL in the layers p-GaN. The efficiency reaches a maximum in the vicinity of the bias $V = 2.75$ eV, corresponding to the peak energy of the blue (BL) PL band in the layers p-GaN [1,18], and begins to fall at the bias $V = 2.95$ eV, corresponding to the maximum of the Gaussian $\rho_{\text{BL}}(E)$, slowing down sharply at the bias of $V = 3.15$ eV at its high-energy edge. The curve $\eta(V)$ for the nanostructure B at $V = 2.4$ eV corresponding to the maximum of the Gaussian $\rho_{\text{YL}}(E)$ has a concavity (deflection) and at $V = 2.6$ eV corresponding to the maximum of the Gaussian $\rho_{\text{GL}}(E)$, also has a maximum.

Humps on the curves $\eta(V)$ occur when the level E_{tp} intersects wide impurity bands (full width at half height FWHM $\approx .4$ eV) color centers $\rho_{if}(E_{\text{tp}})$, due to a change in the tunnel resistance of the well wall r_{w}, causing a change in the distribution of the voltage increment between the injection barrier and the well wall.

With an increase in the bias in the area $V \le V_{\text{p}}$, the density of states $\rho_{if}(E_{\text{tp}})$ and $\rho_{\text{Uf}}(E_{\text{tp}})$ increases at the level of E_{t} at $E_{\text{tp}} < E_{0i}$ causes a decrease in r_{w} and a greater decrease in the injection barrier, which manifests itself in the growth of I_{EL} and η. The recharge of the states $\rho_{if}(E_{\text{tp}})$, which reduces the electric field strength in the well wall, as well as a decrease in their density at $E_{\text{tp}} > E_{0i}$, causes an increase in r_{w} and a smaller decrease in the barrier, which is reflected in a slowdown in the growth of I_{EL} and η with an bias. For $V > V_{\text{p}}$, on the contrary, a decrease in r_{w} leads to a slower drop in η with an increase in bias, and an increase in r_{w} — leads to a faster drop η. Since the Gaussian distribution has an inflection point at half the height of the peak, where $d\rho_{if}(E)/dE$ is maximal, in the case of $\rho_{if}(E_{\text{tp}}) > \rho_{\text{Uf}}(E_{\text{tp}})$ when the level of E_{tp} intersects the Gaussian impurity zone in the region of $E_{\text{tp}} < E_{0i}$ on the curve $\eta(V)$ there is a bulge (hump). Since $d\rho_{\text{Uf}}(E)/dE$ grows with the increase of E, in the case of $\rho_{\text{Uf}}(E_{\text{tp}}) > \rho_{if}(E_{\text{tp}})$,a concavity (deflection) occurs on the curve $\eta(V)$. In the case $\rho_{\text{Uf}}(E_{\text{tp}}) \approx \rho_{if}(E_{\text{tp}})$ a double hump appears on the curve $\eta(V)$: a hump in the region of the Gaussian increase $\rho_{if}(E)$, at $E_{\text{tp}} > E_{0i}$, caused by the growth of states $\rho_{if}(E_{\text{tp}})$ and their recharging, and a secondary hump in the region of the Gaussian decline $\rho_{if}(E)$, at $E_{\text{tp}} > E_{0i}$, due to the growth of states $\rho_{\text{Uf}}(E_{\text{tp}})$, but the decrease and recharge of states $\rho_{if}(E_{\text{tp}})$.

In the structure A, the relatively low density of states of the Urbach tail $\rho_{\text{U}}(E)$ provides low tunneling permeability and conductivity of the p-barrier. The tunnel leakage current at the threshold bias is small and is 0.2 μA. Near the threshold bias, the contributions of the states $\rho_{\text{YL}}(E)$ and $\rho_{\text{U}}(E)$ to the total density of unoccupied final states are comparable. In the region $V = 2.2{-}2.6$ eV, when the level E_{tp} crosses the impurity band of the YL color centers, on the curve $\eta(V)$ in the peak region ofYL-Gaussian, near $V = 2.4$ eV, a distinct concavity (deflection) appears after the convexity (hump), a secondary hump appears on the decline of the YL-Gaussian, near $V = 2.5$ eV, on the curve $\eta(V)$. The decrease in tunnel permeability caused by a significant decrease in the charge in the well wall when recharging YL centers leads to a decrease in the contribution of the states $\rho_{\text{GL}}(E)$, $\rho_{\text{BL}}(E)$ and $\rho_{\text{U}}(E)$ into tunneling conductivity and slows down efficiency growth with the bias increase at $V < V_{\text{p}}$ and its droop at $V > V_{\text{p}}$.

In the structure B, the high density of states of the Urbach tail $\rho_{\text{U}}(E)$ provides high tunneling permeability and conductivity of the p-barrier. The tunnel current at the threshold bias, equal to 4 μA, is more than an order of magnitude higher than the current in the structure A. The contribution of the states of the color centers to the total density of unoccupied final states $\rho_{\text{f}}(E_{\text{tp}})$ is small, and the rapid growth of I_{rad} and I_{EL} with increasing voltage in the region $V = 2.2{-}2.6$ eV is provided by the exponential growth of $\rho_{\text{U}}(E_{\text{t}})$. Overcharging of the YL color centers leads to a decrease in the contribution of the states $\rho_{\text{U}}(E_{\text{t}})$ to the tunnel conductivity and manifests itself in the concavity (deflection) of the curve $\eta(V)$ near $V = 2.4$ eV. Overcharging of the GL color centers leads to an increase in the current $I_{\text{n/rad}}$, causing a drop in efficiency.

3.5. The effect of the recharge of the color centers on spectral efficiency EL

To confirm these model considerations, we have made measurements of the partial quantum efficiency of radiation in various parts of the EL spectrum. Fig. 3 illustrates the behavior of the emission efficiency of photons with energy $h\nu$ with the forward bias increase in the structures A and B. The spectral efficiency of $\eta_{h\nu}(V) \equiv I_{h\nu}(V)/I(V)$ can be defined as equal to the number of emitted photons with energy $h\nu$ when one electron flows in the external circuit ($I_{h\nu}$ — spectral intensity of radiation). The dependences $\eta_{h\nu}(V)$ are obtained from a series of spectra measured at various forward biases.

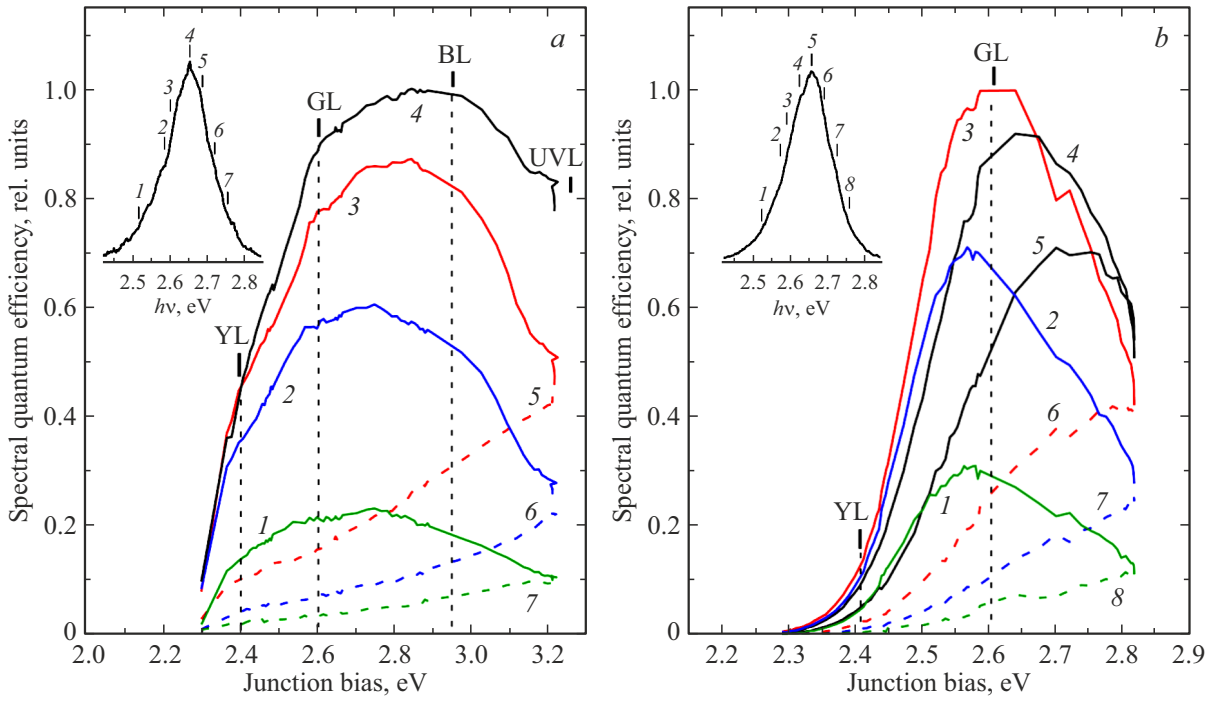

Figure 3. The dependences of the spectral efficiency of the EL from the forward bias $\eta_{h\nu}(V)$ for the structures A (a) and B (b). The values of peak efficiencies are normalized. The energy of the emitted photon, eV: a) *1* — 2.52, *2* — 2.58, *3* — 2.6, *4* — 2.65, *5* — 2.69, *6* — 2.72, *7* — 2.75; b) *1* — 2.52, *2* — 2.58, *3* — 2.6, *4* — 2.63, *5* — 2.66, *6* — 2.69, *7* — 2.72, *8* — 2.75. On the inserts — EL spectra $I_{h\nu}(h\nu)$ at $I = 20$ mA for the structures A (a) and B (b), the markers highlight the energies of the emitted photons for the curves $\eta_{h\nu}(V)$ with the corresponding numbers.

From Fig. 3 it can be seen that with equal spectral efficiency of radiation with energy $h\nu < h\nu_p = 2.65$ eV and $h\nu > h\nu_p$ at rated current 20 mA, in the region of peak bias, the efficiency of low-energy radiation is 4–5 times greater, and its dependence on bias has a maximum, whereas the increase in the efficiency of high-energy radiation with the bias only slows down in the region of $V > V_p$.

Comparison of curves $\eta_{h\nu}(V)$ (Fig. 3) and $\eta(V)$ (Fig. 2, b, and curves *3* and *3′*) shows, that the on the curves $\eta_{h\nu}(V)$ appear in the regions of the same forward biases as on the curves $\eta(V)$. This fact is consistent with the notion that carriers tunneling into the quantum well are thermalized into states of Urbach tails $\rho_U(E)$ in InGaN, and the probability of filling states with different localization energies E_{loc} is proportional to their density [9,19–21]. The asymmetric shape of the emission spectrum, which is characteristic of disordered materials with a sharper on a high-energy wing is associated with the fact that part of the carriers captured into states with energy $E > h\nu_p$ does not have time to recombine radiatively. It is assumed that in the case of a relatively low density of states $\rho_U(E)$ and the absence of carrier hops between local centers, carriers are thermally ejected to the mobility edge and re-captured, evenly filling the states of the zone tails [22,23]. In the case of high density states $\rho_U(E)$ the role of the mobility edge is played by the demarcation level, and carriers from shallow states are thermalized into deeper states by tunnel hops between tail states [24,25].

As can be seen from Fig. 3, the type of dependences on the bias of the radiation efficiency for states with different localization energies is significantly different.

In the structure A for electrons trapped in deep states in the quantum well emitting photons with energy $h\nu < h\nu_p$, the density of isoenergetic final states $\rho_{Uf}(E)$ in the well wall decreases with increasing localization energy E_{loc} proportionally to $\exp(-E_{loc}/E_U)$ (Urbach parameter $E_U > kT$), but the rate of nonradiative recombination of an electron and a hole increases faster as $\exp(E_{loc}/kT)$. As a result, the depth of localization of carriers in the quantum well is compensated by a higher rate of nonradiative recombination through deep isoenergetic states of tails in the well wall. Recharging YL centers leads to a greater outflow of electrons from deep states. As a result, the efficiency of radiation with lower energy $h\nu$ weakly increases with increasing V and at smaller biases begins to decrease, approaching the efficiency at $V = 2.4$ eV, before the start of recharging YL centers. With an increase in the radiation energy $h\nu$ in the region $h\nu < h\nu_p$, the inflection of the curves $\eta_{h\nu}(V)$ near the maxima of the Gaussians YL- and GL-centers becomes weaker, the maximum spectral efficiency shifts towards large biases, the drop of $\eta_{h\nu}$ decreases as the bias increasing (Fig. 3, a, curves *1–4*). As a result, at biases $V > V_p$, the spectral efficiency of radiation on the low-energy wing of the EL spectrum decreases with the bias increase, which is reflected in the blue shift of the

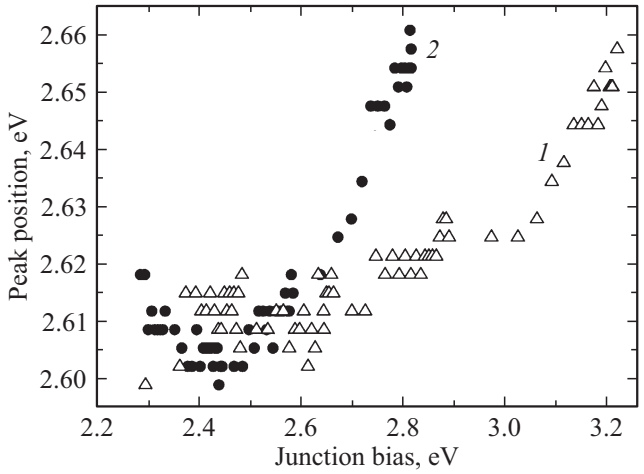

Figure 4. Spectral position of the peak of the EL spectrum as a function of forward bias for structures A (*1*) and B (*2*).

peak of the radiation spectrum accompanying a decrease in the efficiency of the EL (Fig. 4, curve *1*). At a rated current of 20 mA, the blue shift of the spectrum peak reaches 50 MeV.

For the electrons trapped in small tail states emitting photons with energy $h\nu > h\nu_{\mathrm{p}}$, the density of final states $\rho_{\mathrm{Uf}}(E)$ for the electrons tunneling from a quantum well, it is large enough, and the distance between the centers is small. Due to the exponential dependence of the electron jump rate on the distance between local centers proportional to $\exp(-E_{\mathrm{loc}}/E_{\mathrm{hop}})$ ($E_{\mathrm{hop}} < kT$ — characteristic energy of jump thermalization), the electron leaves the center faster than it can recombine, which increases the tunneling outflow of electrons with low energy E_{loc} through the wall of the quantum well. As the bias increases, the recharge of the YL-, GL- and BL- color centers leads to an increase in the tunnel resistance of the well wall and forward on the wall, accompanied by an increase in the density of the isoenergetic final states $\rho_{\mathrm{Uf}}(E)$ for electrons tunneling out of the quantum well and their tunneling outflow through the wall, which manifests itself in a slowdown in the growth of spectral efficiency with with increasing bias (curves *5*–*7*), as well as in the broadening of the emission

In the structure B, the high density of states of the Urbach tail $\rho_{\mathrm{Uf}}(E)$ provides high tunneling permeability and conductivity of the p-barrier, and, accordingly, a large tunneling leakage current under the quantum well and from the quantum well. The recharge of YL centers reduces the tunneling permeability and the contribution of the states $\rho_{\mathrm{Uf}}(E)$ to the tunneling conductivity, and at $V = 2.4$ eV, the spectral efficiency of emission at the low-energy edge of the spectrum is very small (Fig. 3, *b*, curve *1*). But after the E_{tp} level crosses the maximum of the Gaussian of YL-centers, when the accumulation of neutralized YL-centers slows down, the exponential growth of the states of $\rho_{\mathrm{Uf}}(E)$ begins to outpace the decrease in tunnel permeability and the spectral efficiency increases rapidly with increasing bias the offset increase (curves *2* and *3*), leading to a red shift of the maximum of the emission spectrum by 20 meV at low bias (Fig. 4, curve *2*). The recharge of GL centers and an increase in the forward bias on the well wall leads to a sharp increase in the tunneling electron flux from the quantum well, a decrease of η for centers emitting photons with energy $h\nu \geq 2.6$ eV and a blue shift in the emission spectrum at $V > V_{\mathrm{p}}$, amounting to 60 MeV at a rated current of 20 mA.

4. Conclusion

In p–n-nanostructures with the InGaN|GaN quantum well, ionized deep centers make a significant contribution to the volume charge density and electric field strength in the potential walls of the quantum well, which increases their tunneling permeability and lowers the injection barrier, allowing the main carriers to tunnel into the quantum well and thermalize into the states of the Urbach tails of the well. The recharge of the color centers in the well wall in the p-barrier as the forward bias increases leads to a decrease in the tunneling permeability of the wall and an increase in the drop in direct voltage on the wall, which, in turn, leads to an increase in the tunneling outflow of non-basic carriers (electrons) from the quantum well due to an increase in the density of isoenergetic local centers in the well wall.

The maximum efficiency of localization and radiative recombination of carriers in a quantum well is achieved when, with an increase in the injection level, the differential resistances of the well wall and the injection barrier become equal. In the case of a comparable density of color centers and states of Urbach tails in the well wall, the decrease in localization efficiency with the bias increase and recharge of color centers is mainly due to an increase in the rate of nonradiative recombination in the well wall. In the case of the predominance of the density of states of the Urbach tails, an increase in the velocity of tunneling electron jumps between local centers in the wall of the well dominates.

Conflict of interest

The authors declare that they have no conflict of interest.

References

[1] S. Nakamura, G. Fasol. The Blue Laser Diode: GaN Based Light Emitters and Lasers. Springer (1998).
[2] D. Feezell, S. Nakamura. Comptes Rendus Physique **19**, *3*, 113 (2018).
[3] C.H. Qiu, C. Hoggatt, W. Melton, M.W. Leksono, J.I. Pankove. Appl. Phys. Lett. **66**, *20*, 2712 (1995).
[4] O. Ambacher, W. Reiger, P. Ansmann, H. Angerer, T.D. Moustakas, M. Stutzmann. Solid State Commun. **97**, *5*, 365 (1996).
[5] P. Perlin, M. Osinski, P.G. Eliseev, V.A. Smagley, J. Mu, M. Banas, P. Sartori. Appl. Phys. Lett. **69**, *12*, 1680 (1996).
[6] J.R. Lang, N.G. Young, R.M. Farrell, Y.R. Wu, J.S. Speck. Appl. Phys. Lett. **101**, *18*, 181105 (2012).

[7] H. Zhang, E.J. Miller, E.T. Yu. J. Appl. Phys. **99**, *2*, 023703 (2006).
[8] L. Esaki. Tunneling phenomena in solid states (Tunnel'nyye yavleniya v tverdykh telakh) / Ed. V.I. Perel. Mir, M. (1973). [In: Tunneling phenomena in solids / Eds E. Burstain, S. Lundqvist. Plenium Press, N.Y. (1969). Ch. 5].
[9] S.F. Chichibu, Y. Kawakami, T. Sota. In: Introduction to Nitride Semiconductor Blue Lasers and Light Emitting Diodes / Eds S. Naramura, S.F. Chichibu. Taylor & Francis, L. and N.Y. (2000). Ch. 5.
[10] N.I. Bochkareva, A.M. Ivanov, A.V. Klochkov, Y.G. Shreter. J. Phys.: Conf. Ser. **1697**, 012203 (2020).
[11] M.A. Reshchikov, H.J. Morkoç. J. Appl. Phys. **97**, *6*, 061301 (2005).
[12] N.I. Bochkareva, Yu.G. Shreter. FTT **64**, *3*, 371 (2022). (in Russian).
[13] S. Nakamura, M. Senoh, N. Iwasa, S. Nagahama, T. Yamada, T. Mukai. Jpn J. Appl. Phys. **34**, *10B*, L1332 (1995).
[14] Y.T. Rebane, N.I. Bochkareva, V.E. Bougrov, D.V. Tarkhin, Y.G. Shreter, E.A. Girnov, S.I. Stepanov, W.N. Wang, P.T. Chang, P.J. Wang. Proceed. SPIE **4996**, 113 (2003).
[15] A. David, M.J. Grundmann, J.F. Kaeding, N.F. Gardner, T.G. Mihopoulos, M.R. Krames. Appl. Phys. Lett. **92**, *5*, 053502 (2008).
[16] A.G. Chynoweth, W.L. Feldmann, R.A. Logan. Phys. Rev. **121**, *3*, 684 (1961).
[17] L.V. Keldysh. ZhTF **33**, *4*, 994 (1957); **34**, *4*, 962 (1958). (in Russian).
[18] S.F. Chichibu, A. Uedono, K. Kojima, H. Ikeda, K. Fujito, S. Takashima, M. Edo, K. Ueno, S. Ishibashi. J. Appl. Phys. **123**, *16*, 161413 (2018).
[19] C. Gourdon, P. Lavallard. Phys. Status Solidi B **153**, *2*, 641 (1989).
[20] A.A. Klochikhin, S.A. Permogorov, A.N. Reznitsky. FTT **39**, *7*, 1170 (1997). (in Russian).
[21] N.I. Bochkareva, I.A. Sheremet, Yu.G. Shreter. FTP **50**, *10*, 1387 (2016). (in Russian).
[22] T. Tiedje, A. Rose. Solid State Commun. **37**, *1*, 49 (1980).
[23] D. Monroe. Phys. Rev. Lett. **54**, *2*, 146 (1985).
[24] Y. Narukawa, Y. Kawakami, S. Fujita, S. Fujita, S. Nakamura. Phys. Rev. B **55**, *4*, R1938 (1997).
[25] S.F. Chichibu, H. Marchand, M.S. Minsky, S. Keller, P.T. Fini, J.P. Ibbetson, S.B. Fleischer, J.S. Speck, J.E. Bowers, E. Hu, U.K. Mishra, S.P. DenBaars, T. Deguchi, T. Sota, S. Nakamura. Appl. Phys. Lett. **74**, *10*, 1460 (1999).